Received: 20 July 2022 | Revised: 6 September 2022 | Accepted: 17 September 2022

DOI: 10.1111/jace.18804

Journal of the American Ceramic Society

RESEARCH ARTICLE

Reactive flash sintering in a bilayer of zirconia and lanthana: Measurement of the diffusion coefficient in real time

Syed I. A. Jalali[1] | **Rishi Raj**[1,2]

[1]Department of Mechanical Engineering, University of Colorado Boulder, Boulder, Colorado, USA

[2]Materials Science and Engineering Program, College of Engineering, University of Colorado Boulder, Boulder, Colorado, USA

Correspondence
Rishi Raj, Department of Mechanical Engineering, University of Colorado Boulder, Boulder, CO 80309, USA.
Email: rishi.raj@colorado.edu

Funding information
Office of Naval Research, Grant/Award Number: N00014-18-1-2270

Editor's Choice
The Editor-in-Chief recommends this outstanding article.

Abstract

Reactive flash sintering is a process where off-the-shelf powders of elemental oxides can be simultaneously sintered and reacted to form a multicomponent oxide in a matter of seconds at low furnace temperatures. The fact that several cation species, each residing within their own particles, can migrate over distances of several micrometers, and mix on the atomic scale to form multicomponent oxides, so quickly, is quite remarkable. The question arises as to the rate of this solid-state diffusion phenomenon. In this paper, we present measurements of this diffusion coefficient from live flash experiments. The results are obtained from millimeter scale bilayers of yttria-stabilized zirconia and lanthana where the flash initiates in the zirconia layer and then migrates into the lanthana layer, forming lanthanum zirconates. The velocities of migration of the flash-front, coupled with measurements of the length scale of the profile of zirconium and lanthanum interdiffusion, across the bilayer interface, provide an estimate of the effective diffusion coefficient. These measurements give a value for the cation diffusion to lie in the range of 2.5×10^{-10} m^2 s^{-1} at 1380°C, with an activation energy of 200–250 kJ mol^{-1}. In comparison, the cation diffusion coefficient in yttria-stabilized zirconia, at 1350°C, is stated to be 1.1×10^{-20} m^2 s^{-1} with an activation energy of ~550 kJ mol^{-1}. A pause for reflection.

KEYWORDS
diffusion, lanthanum oxide, reactive flash sintering, zirconia

1 | INTRODUCTION

The original exposition of flash sintering, carried out on yttria-stabilized zirconia a decade ago, has since been expanded to many if not all oxides as described in an expansive review by Yu et al.[1] and partly summarized in Ref. [2]. The method of flash sintering was originally reviewed by Dancer.[3] More recent review papers include Biesuz and Sglavo[4] and Guillon et al.[5] A collection of papers in a recent issue of the MRS Bulletin presents state-of-the-art concepts and views on this topic.[6] A history of flash sintering has been described by Pérez-Maqueda et al.[7] These reviews affirm the generality of the flash method for sintering of ceramics, where sintering can occur in mere seconds at unusually low furnace temperatures by the application of modest electrical fields, typically 100 V cm^{-1}, and current densities in the range of 100 mA mm^{-2}.

Flash experiments are generally carried out in two ways. In voltage-to-current experiments, flash is induced by a combination of electric field and furnace temperature (in either isothermal or constant heating rate modes); the power supply is switched to current control at the onset of flash to limit thermal runaway.[8]

Alternatively, in so-called current-rate experiments,[9] current is injected directly into the specimen that is held at a constant temperature. The onset of flash, which causes a sharp increase in conductivity, is signaled by a peak in the voltage expressed across the specimen. The advantage of current-rate experiments is that the time for sintering can be stretched from a few seconds to several minutes by changing rate at which the current is ramped up, thereby affording greater control of the process. In these experiments, it was discovered that the sinter density was independent of the current rate; it was related only to the instantaneous values of the current density[9]—why this is so remains a wide-open question in the science of flash sintering.

In this article, we have used the voltage-to-current method. In this method, the flash effect is described by three stages[8]: the run up to the onset of flash (I), the transition to current control (II), and holding the specimen at constant current (III). We study the migration of flash in Stage III in a two-phase, bilayer ceramic system.

In a recent paper,[10] we have described the migration of flash in a bilayer constructed from two ceramics that do not react: 8 mol% yttria-stabilized zirconia and alumina. Each ceramic, on its own, has quite different requirements for the induction of flash. For example, yttria-stabilized zirconia flashes below 800°C at a field of ~100 V cm^{-1}, whereas alumina requires greater than 1300°C at more than 1000 V cm^{-1}. It was shown that in these bilayers, where each layer stretched across to both electrodes, the flash initiated in the zirconia layer but then migrated transversely into the alumina layer, causing it to sinter. In this way, alumina could be sintered at field and temperature appropriate for 8YSZ. We have called this phenomenon catalytic flash sintering because zirconia catalyzes sintering in alumina at unusually low field and temperature. In these zirconia/alumina experiments, chemical analysis across the interface did not show any interdiffusion of zirconium into alumina consistent with the mutual insolubility of these compounds. Thus, the migration of flash was concluded to have an electronic nature.

The motivation for present experiments arose from the recently reported phenomenon of "reactive flash sintering" (RFS). For example, it was shown, for the first time,[11] that flash experiments with powder mixtures of bismuth oxide and ferric oxide yielded single-phase, fully sintered bismuth ferrite in a few seconds at low furnace temperatures at modest electrical fields. Later, the method was applied to the synthesis of alumina-doped lithium–lanthanum–zirconate, $Li_{6.25}Al_{0.25}La_3Zr_2O_{12}$ (Al–LLZO), from powders of lithia, lanthana, zirconia, and alumina[12], a leading candidate for the electrolyte in solid-state lithium–ion batteries. Here, the short time of RFS processing was especially important because the loss of lithium in the conventional sintering poses a very significant technical barrier.[13]

The speed of RFS is unusual, because the cations must migrate from the parent powder particle to mix atomistically with cations from other powders to form a single-phase multicomponent ceramic. Apparently, the rate of solid-state interdiffusion in RFS is anomalously rapid.

The objective of the present experiments was to obtain a measurement of the coefficient for interdiffusion in RFS from measurements of the migration of the flash in bilayers of 8YSZ/La_2O_3 in real time. The migration of flash is accompanied by the formation of a lanthanum zirconate alloy.

(i) We present several results from the previous 8YSZ/La_2O_3 experiments.
(ii) The flash is established quickly in the 8YSZ layer and after a brief pause migrates into the adjacent La_2O_3; the total time before the entire sample is engulfed in flash is less than 4 s.
(iii) The analysis of the velocity of migration of the flash suggests an interface-controlled mechanism, most likely electronic in nature.
(iv) Measurements of the shrinkage strain as a function of time shows that sintering lags the migration of flash.
(v) The experiments are carried out in two ways: (i) by allowing the specimen to cool down in the furnace when all the furnaces and the flashes are turned off, and (ii) by moving the specimen from the furnace and submerging it into liquid nitrogen in the in-flash condition and then quenching it by turning off the flash. The EDS profiles show the formation of precipitates in the furnace-cooled specimen and an apparent solid solution in the LN_2-quenched sample.
(vi) The width of the reaction zone in LN_2-quenched specimens is measured as a function of temperature by increasing the current density from 100 to 200, and then to 300 mA mm^{-2}. This permits an estimate of the activation energy. The activation energy is a fraction of the activation energy obtained in conventional deformation experiments, where the rate of deformation is related to solid-state diffusion.[14] The present low value is consistent with recently reported in-flash superplastic-deformation experiments.[15]

2 | EXPERIMENTAL PROCEDURES

Tetragonal zirconia (3 mol% yttria-stabilized zirconia—3YSZ) powder (TZ–3YS–B grade powder) was obtained from Tosoh Corp., Shunan, Japan, and 99.9% pure lanthanum oxide powder was purchased from Alfa Aesar. Both powders had the premixed binder in the as received condition. The powders were pressed into dogbones by layering and pressing uniaxially with a pressure of 28 MPa. The total thickness of the bilayer was ~1 mm, each layer being ~0.5 mm thick.

The sintering experiment was carried out in a horizontal tube furnace that provided access to the camera (Imaging Source DMK23G274) and optical spectrometer (Ocean Optics USB-6000) and a pyrometer (Micro Epsilon model CTLM-1HCF4-C3). After placing the green bilayer within the tube, the furnace was heated at a constant rate of 10°C min^{-1} until it reached the desired temperature of 800°C. Bilayer specimens were supported within the furnace with Kanthal wires threaded into the holes at the ends of the dogbone specimens. Contacts were coated with silver paste to improve the uniformity of current flow through the gage section.

The experiments were initiated in voltage control mode in a range of 100–700 V cm^{-1}. The onset of flash was signaled by an abrupt rise in conductivity. At this point, the power supply was switched to current control. Three separate experiments with the current limits set to 100, 200, and 300 mA mm^{-2} were done to measure the temperature dependence of the diffusion coefficient.

The sequence of flash was as follows: The zirconia layer flashed first, which was followed by a brief pause, followed by the migration of the flash front in the thickness direction into the lanthana layer. Time lapse pictures of the migration of flash were obtained at the rate of 10 frames per second.

For the characterization of the chemical profiles by SEM–EDS, two different sets of experiments were performed: (i) furnace cooling with the current to the specimen, and the power to the furnace and to the specimen, turned off, and (ii) in-flash immersion-and-quench in liquid nitrogen as described in Ref. [16], where the specimen is immersed into LN_2 while still in a state of flash (Stage III), and then the power is turned off to quench the structure. The first set showed the evolution of precipitates, whereas the LN_2-quenched samples gave uniform chemical profiles of constituents, as would have existed in the state of flash. The latter method gave a clearer measure of the interdiffusion distance of zirconium and lanthanum.

The X-ray diffraction data were obtained on a Bruker XRD machine. The samples were ground into a powder for these measurements.

3 | RESULTS

3.1 | Typical electrical behavior and electroluminescence

In this section, we report the features of the bilayer experiments. They include plots of voltage (electric field) and current (current density) with time with the furnace held at a constant temperature[8] and electroluminescence.[17]

The voltage and current profiles are shown in parts (A) and (B) of Figure 1, respectively. The figures include data for specimens constructed from (i) powders of 3YSZ, (ii) powders of La_2O_3, and (ii) bilayer specimens (as shown in Figure 1C). The time clock data are synchronized to the onset of flash (that is at 20 s in Figure 1A). The furnace was held at 800°C. Note that the field required to trigger the flash in La_2O_3 is six times that for 3YSZ. However, the bilayer flashes at an intermediate field. It is noticeable that in all three cases, once the current rises to its limit set at the power supply (100 mA mm^{-2}), the steady state for all three cases is the same: about 40–50 V cm^{-1}.

In Figure 1B, the current is seen to rise significantly during Stage I in zirconia before the current rises quickly up to the limit. This increase in current during the incubation period was also present in lanthana, although not as distinctly as in zirconia.

Electroluminescence is another feature of flash experiments.[17] The optical emission has been shown to have an electronic nature because the emission peak remains stationary when the sample temperature is increased[18] (in the case of black body radiation, there is a blueshift at increasing temperatures). The emission spectra from the bilayer, progressing with time, are shown in Figure 2A. The emission from the bilayer is compared with zirconia in Figure 2B. The bilayer shows greater intensity at shorter wavelengths. We do not have enough understanding of the electronic structure in the state of flash to explain this behavior. The energy levels introduced by flash have been measured by optical spectroscopy in single-phase ceramics, such as zirconia[18] and, more recently, in titania. Evidently, flash introduces energy levels just below the conduction band creating a bandgap corresponding to the peak in electroluminescence (at just below 2 eV). Thus, it is likely that the emission arises from the recombination of electrons and holes corresponding to this bandgap, which is in agreement with the peak in the emission spectrum as measured in single-crystal cubic zirconia.[18] It is certainly conceivable that energy levels with a larger bandgap are introduced into lanthanum zirconate or even into lanthana by the flash. Measurement of these energy levels in the state of flash and their understanding from first-principles calculations

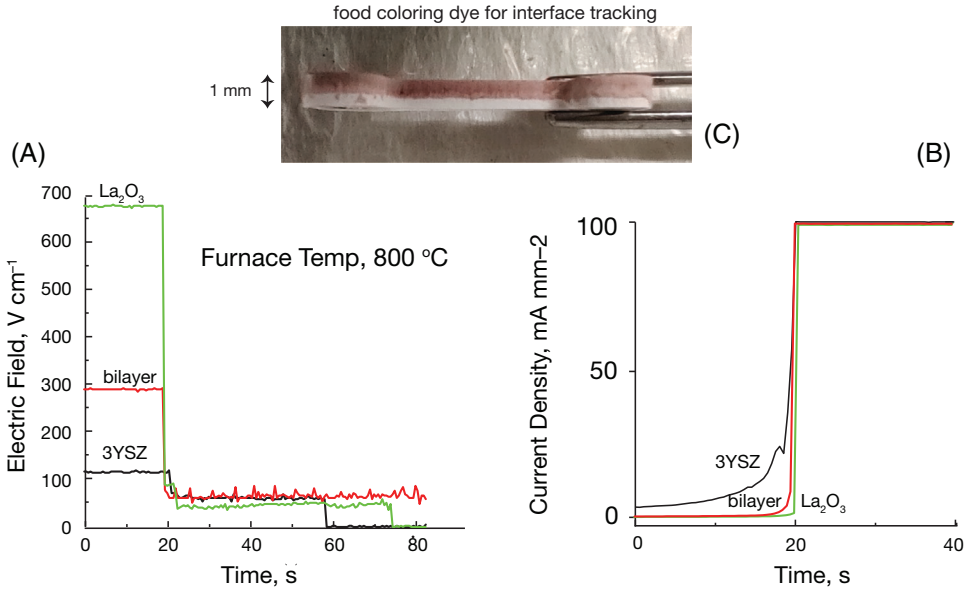

FIGURE 1 (A) and (B) Voltage and current profiles for three types of experiments, plotted from the onset of flash onward; (C) optical micrograph of the "green" bilayer specimen where food coloring was added to the top layer of La_2O_3 to highlight the interface with the zirconia layer underneath

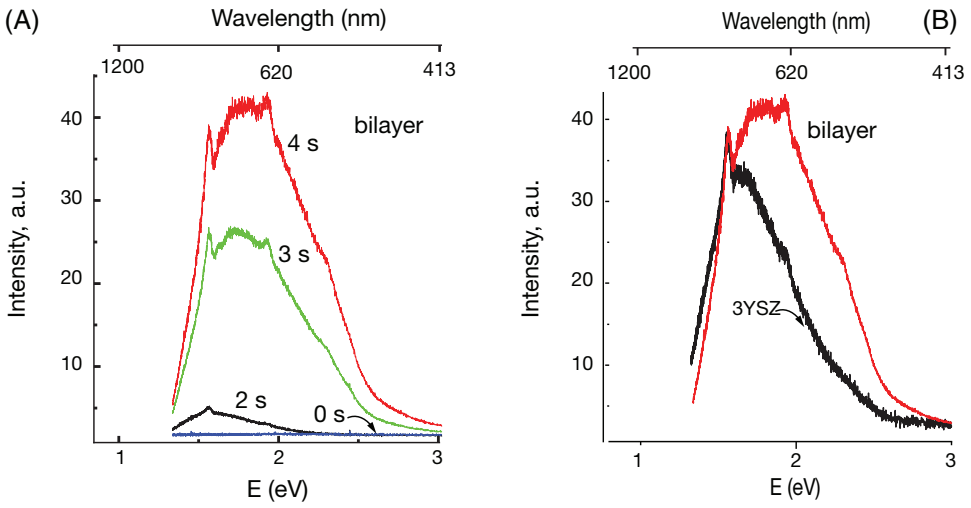

FIGURE 2 Electroluminescence spectra from the bilayer by itself (A), and in comparison with the emission from zirconia (B)

still remain an objective for a deeper understanding of the flash phenomenon.

3.2 | Flash migration and shrinkage measured in real time

Estimation of the diffusion coefficient requires time-dependent migration of atom species. In the bilayer experiment, this information is obtained by measuring the time for the migration of the flash from the zirconia layer (which flashes first) into the lanthana layer, and then measuring the diffusion distance from chemical profiling of the zirconium and lanthanum across the interface. In this section, we report on the migration velocity of the flash from the interface into the lanthana layer.

Time-lapse photographic images of the flash are shown Figure 3. Note that the flash is confined to the middle of the gage length of the dogbone sample, but at the end ($t = 4$ s), it extends into the ears. The flash migration into the La_2O_3 layer is delayed by about 1 s after the zirconia layer has flashed. This is evident from current profile in Figure 3

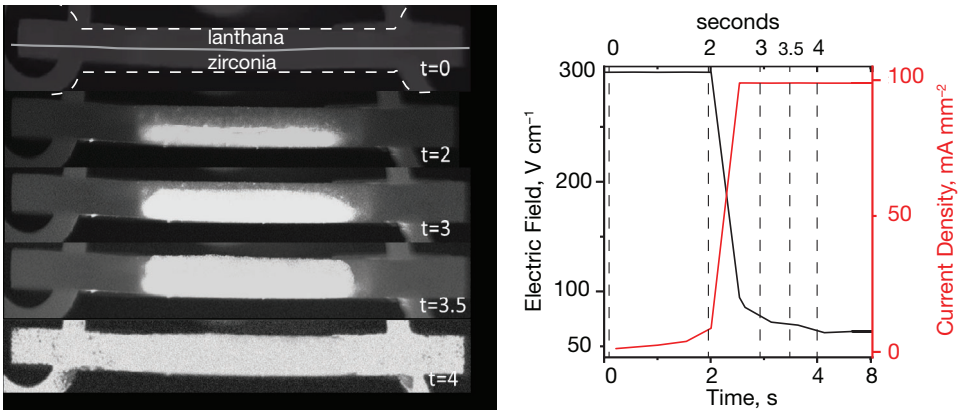

FIGURE 3 Time-lapse photographic images of the migration from flash from the zirconia layer into the lanthana layer

where current rises to the limit over a period of just under 1 s. In conventional flash experiments, the current rises nearly instantaneously at the onset of flash.

The shrinkage strain in the bilayer has two components, the longitudinal strain along the gage length, and the transverse or thickness strain. We must consider that both layers may not necessarily sinter together, and therefore sintering in one layer can constrain the sintering in the other layer.[19] Here, the behavior in conventional and flash sintering are radically different as explained *fundamentally* by Jha and Raj[20]; flash is benign toward differential sintering. As a result, delamination in multilayers during conventional sintering[21] is "obviated" in flash sintering.[22] This fact is of seminal significance in the bilayer experiments. The absence of "constrained sintering" implies that the lanthana layer can continue to sinter without generating interfacial defects even after the zirconia layer underneath has fully sintered. Thus, sintering in the bilayer follows this sequence:

(i) At first, the zirconia layer sinters. However, the in-plane shrinkage is constrained by the lanthana layer just above (at this point, the lanthana layer is porous but functionally rigid). Therefore, the zirconia layer sinters by shrinking predominantly in the in the "z" direction. The remaining sintering in zirconia occurs concomitantly with sintering in lanthana after during the full migration of the flash. These results are displayed in Figure 4A.

(ii) By the time that the lanthana layer begins to sinter, the zirconia layer underneath has nearly sintered. Therefore, the large majority of the shrinkage in lanthana occurs in the thickness direction as seen in Figure 4B.

The time lag between the migration of the flash and the onset of sintering in the lanthana layer is a particularly significant finding. Thus, in Figure 4B, the flash has nearly migrated fully into the lanthana layer when the sintering in lanthana is getting off the ground. Most likely this result is general and probably also occurs in the usual single-phase flash sintering experiments. This result is particularly relevant to touch free sintering where flash plasmas are forced to migrate into a free-standing workpiece by magnetic field.[23] In order to obtain self-similar sintering in three dimensions, it would be necessary for the workpiece to be engulfed in the plasma before it starts to sinter.

3.3 | Coefficient of interdiffusion in the state of flash

The determination of the coefficient for interdiffusion of the cations was separated from the results for migration and sintering as reported in Figure 4. The diffusion measurements were carried out at timescales far beyond 4 s, well into Stage III when the sample is held in a constant state of flash under current control. The Zr and La ions continue to interdiffuse during this time, t. The spatial extent of diffusion, L, is measured from EDS profiles obtained from specimens held for time t in Stage III. The diffusion coefficient, D^*, is then obtained from[24]

$$L^2 = 6D^*t \tag{1}$$

where the temperature dependence of D^* is obtained by increasing the current in Stage III. The temperature is measured with a pyrometer. Experiments were carried out at three current levels: 100, 200, and 300 mA mm^{-2}. The temperatures at these three current levels are shown in Figure 5. This figure also gives the determination of the time, t, spent in Stage III.

The specimens were quenched from the in-flash state into liquid nitrogen by the procedure described in Ref. [16].

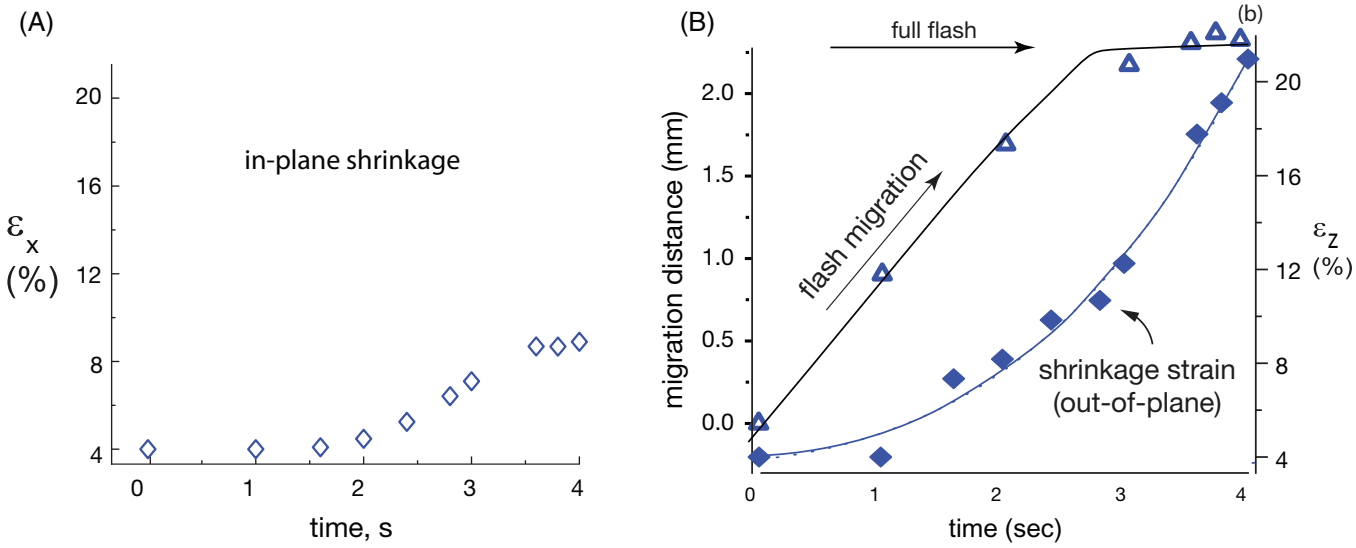

FIGURE 4 (A) In-plane shrinkage, confined to the zirconia layer, measured as a function of time; (B) out-plane shrinkage as well as the migration of the flash from the zirconia into the lanthana layer, as a function of time

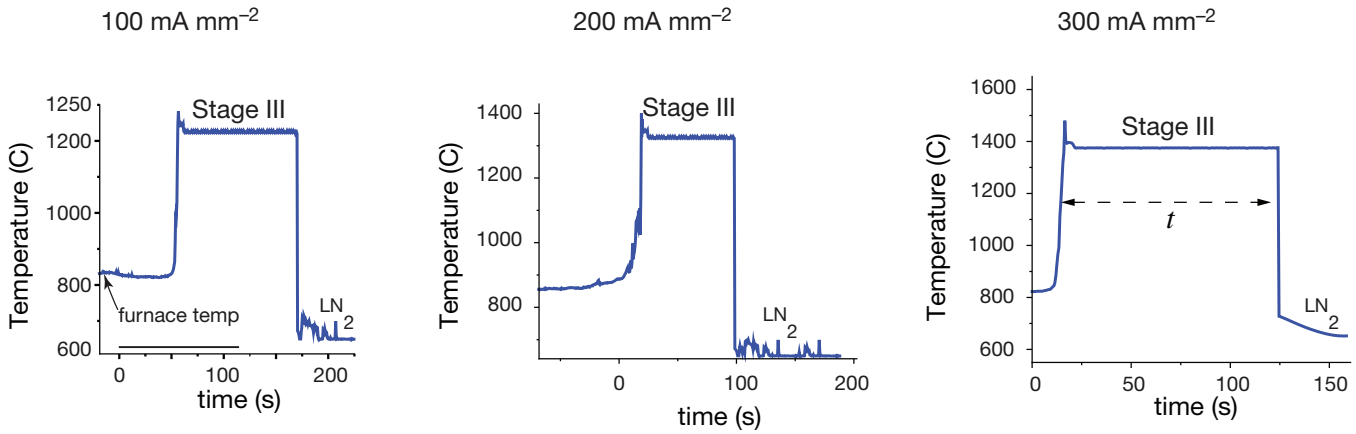

FIGURE 5 The temperature profiles for the specimens held in Stage III at three current levels. These temperatures were used to estimate the activation energy for the coefficient of interdiffusion.

A movie of the in-flash in-immersion specimen showing continued electroluminescence is attached in Supporting Information.

The reason for the liquid nitrogen quench was to prevent the formation of discrete precipitates of lanthanum zirconate in specimens that occurred when the specimens were furnace cooled in air (these results for the air-cooled specimen are included in Section 3.4 on microstructure). The precipitates caused noise in the spatial profiles of La and Zr, which was avoided in LN_2-quenched samples. The EDS profiles for the LN_2 specimens are shown in Figure 6.

The profiles in Figure 6 point toward a mixed diffusion-controlled and interface-controlled behavior. In the case of interface-controlled reaction, the profiles would have a stepwise shape with a sharp change at the edges of, and a uniform concentration within the reaction zone. The profiles of La approximately correspond to such, whereas the Zr profiles are closer to a gradually changing profile within the reaction zone that is closer to diffusion-controlled behavior. We infer that the estimate of D^* from Equation (1) reflects the diffusion coefficient for Zr in the reaction zone.

The time and temperature in Figure 5 and the diffusion length in Figure 6 provide the basis for estimating the diffusion coefficient according to Equation (1). These data are summarized in Table 1.

The calculation in Table 1 shows very high values for the magnitude of the diffusion coefficient: about 10^{-10} m^2 s^{-1} at a temperature of 1300°C. The activation energy, obtained from the Arrhenius plot in Figure 7, is tenuous because

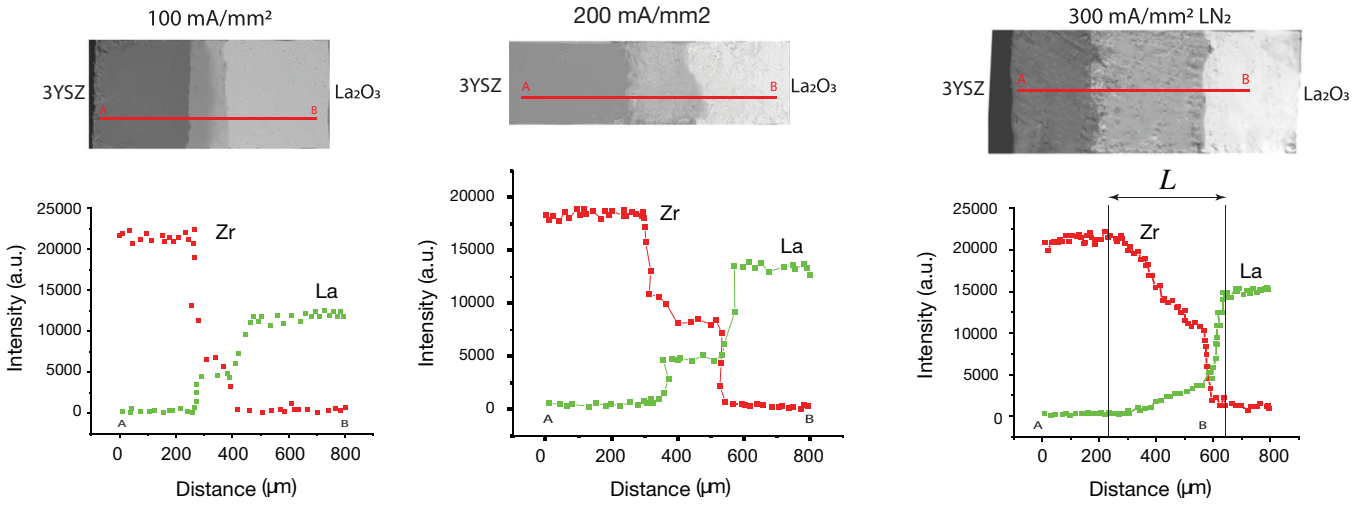

FIGURE 6 Chemical profiles obtained from EDS across the interdiffusion layer in specimens held in Stage III at three temperatures shown in Figure 5

TABLE 1 Measurements of the parameters for Equation (1) at three temperatures, obtained by changing the current density

Current density (mA mm^{-2})	L (μm)	t (s)	T (°C)	D^* (m^2 s^{-1})
100	185	115	1250	5.0E^{-11}
200	260	80	1325	1.4E^{-10}
300	400	105	1380	2.5E^{-10}

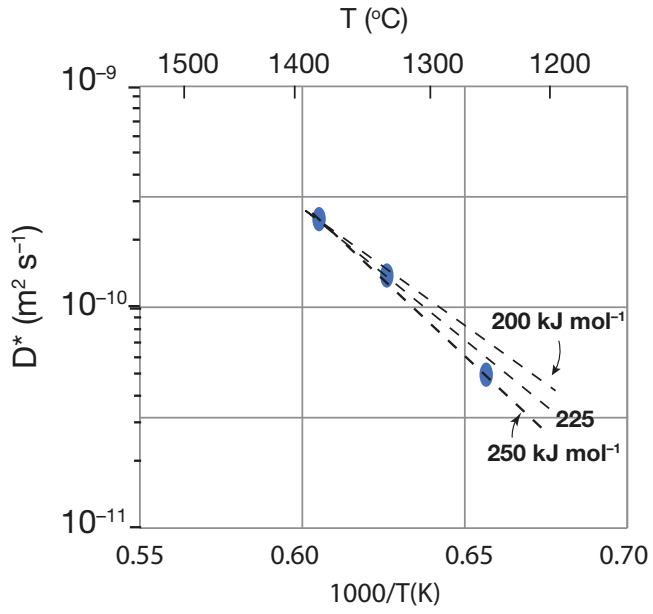

FIGURE 7 The Arrhenius plot for the diffusion coefficient calculated in Table 1. The data show a range in the activation energy from 200 to 250 kJ mol^{-1}, and very high values for the diffusion coefficient.

there are just three data points; still the range of the values, 200–250 kJ mol^{-1}, is significant.

Recently, Motomura et al.[15] studied the kinetics of superplastic deformation in 3YSZ while in an active state of flash. The data were compared with the same experiments carried conventionally without applying current to the specimen. In conventional deformation, they[15] obtained an activation energy of ~550 kJ mol^{-1}, in agreement with the original experiments by Wakai et al.,[14] who had measured activation energies in the range of 570–590 kJ mol^{-1}. However, the activation energy for similar deformation in the state of flash was 200 kJ mol^{-1}.[15] The similarity with the present measurement of 200–250 kJ mol^{-1} is intriguing. It points toward flattening of the activation barrier for diffusion in the state of flash.

The very high values of the diffusion coefficient (10^{-10} m^2 s^{-1} at a temperature of 1300°C) in Table 1 bear a discussion. Kilo et al.[25] measured cation diffusion in yttria-stabilized zirconia by tracer diffusion with a value of 1.1×10^{-20} m^2 s^{-1} at 1350°C. They also addressed the variability in the measurement of cation diffusion, which give a range within two orders of magnitude of 1.1×10^{-20} m^2 s^{-1}. The present measurement is more than six orders of magnitude faster than tracer diffusion data.

More on this topic is described in the following section.

3.4 | Microstructure

Here we report on the grain size in the bilayer specimens sintered by flash. The grain size shows a sharp transition from being a fine grain size in zirconia to a coarse

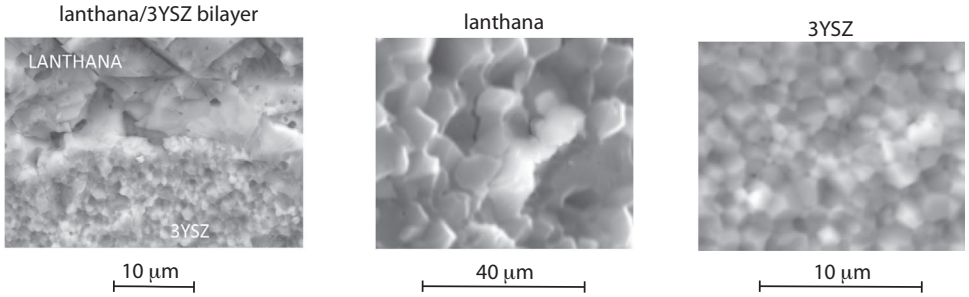

FIGURE 8 Micrographs of grain size in the zirconia and the lanthanum zirconate layers flashed at 100 mA mm^{-2} followed by LN_2 quench. The particle size of lanthanum oxide powder and the 3YSZ powder was 30–50 nm.

grain size in lanthana, as shown in Figure 8. Note that the interdiffusion distance reported in Figure 6 is far greater than the grain size on either side of the interface (the profiles suggest reciprocal interdiffusion, that is, Zr diffuses into lanthana just as well as La diffuses into zirconia).

In the context of Figure 6, it was mentioned that liquid nitrogen quench was needed to prevent the precipitation of lanthanum zirconate compounds, which led to fluctuations in composition profiles (the quenched sample retained a solid solution like character creating distinct boundaries for the interdiffusion zone). Here we report on the microstructure of those precipitates in furnace-cooled specimens. This specimen was flashed at 100 mA mm^{-2}. The compositions at different locations near the interface, as well as the chemical profiles determined by EDS, along with X-ray diffraction data are shown in Figure 9.

In the furnace-cooled sample, region 1 corresponds to the zirconia layer, whereas 2 and 3 lie within the reaction zone. In the LN_2-quenched sample, region 4 belongs to zirconia, and region 6 to the lanthana layer. Thus, 1 and 4 have the composition of yttria-stabilized zirconia, whereas 6 corresponds to lanthana but containing some (with 1.69 wt%) Zr. Region 5 in the LN_2-quenched sample has solid solution mixture of Zr and La corresponding to 13.4 and 71.6 wt%, respectively. Region 3 in the furnace-cooled specimen has approximately the same composition at region 5 in the LN_2-quenched sample.

4 | DISCUSSION

The colossal rates of solid-state diffusion suggested by the phenomenon of RFS are apparently confirmed by measurements of flash migration in bilayers made from zirconia and lanthana. They give cation diffusion to lie in the range of $\sim 2.5 \times 10^{-10}$ m^2 s^{-1} at 1380°C, with an activation energy of 200–250 kJ mol^{-1}. In comparison the cation diffusion coefficient in yttria-stabilized zirconia, at 1350°C is stated to be 1.1×10^{-20} m^2 s^{-1} with an activation energy of ~550 kJ mol^{-1}.[25]

Diffusion rates depend on the packing and bonding among species. For example, higher free volume of liquids leads to much faster diffusion rates. For example, although solid-state diffusion in several metals converges toward 10^{-12} m^2 s^{-1} close to the melting point, the diffusion rate in liquid just beyond the melting point lies between 2×10^{-9} and 6.3×10^{-9} m^2 s^{-1} for most metals because of the increase in specific volume, which is approximately 3% for many metals.[26]

Therefore, the explanation for these very high diffusivities may be related to the free volume in the active state of flash in Stage III.

Indeed, synchrotron experiments have shown lattice expansion in yttria-stabilized zirconia.[27] Preliminary measurements of volume expansion in our laboratory while the specimen is held in Stage III are showing significant volumetric expansion, somewhat approaching the values seen at melting transitions, which have been measured to lie in the range of 3%–4%.[28]

In situ flash experiments in RFS of bismuth ferrite (from powders of bismuth oxide and ferric oxide) carried out at the Brookhaven Synchrotron[29] have shown anomalously large lattice expansion of 3% in the "*a*" direction.

If unusual values of free volume in Stage III of flash are deemed to be responsible for very high diffusivities, the question arises how it can be that the crystalline structure does not melt under flash (as evidenced by live measurements at synchrotrons). We can only speculate at this point. It may be that although melting is a phase transition in the entire specimen arising from the higher entropy of the liquid phase, in the "flash plasma," the increase in entropy may be spatially dispersed. Flash experiments with materials that have a tendency to solidify into a glass from the melt as in metallic glasses (made from eutectic compositions) may indeed yield glasses in flash experiments.

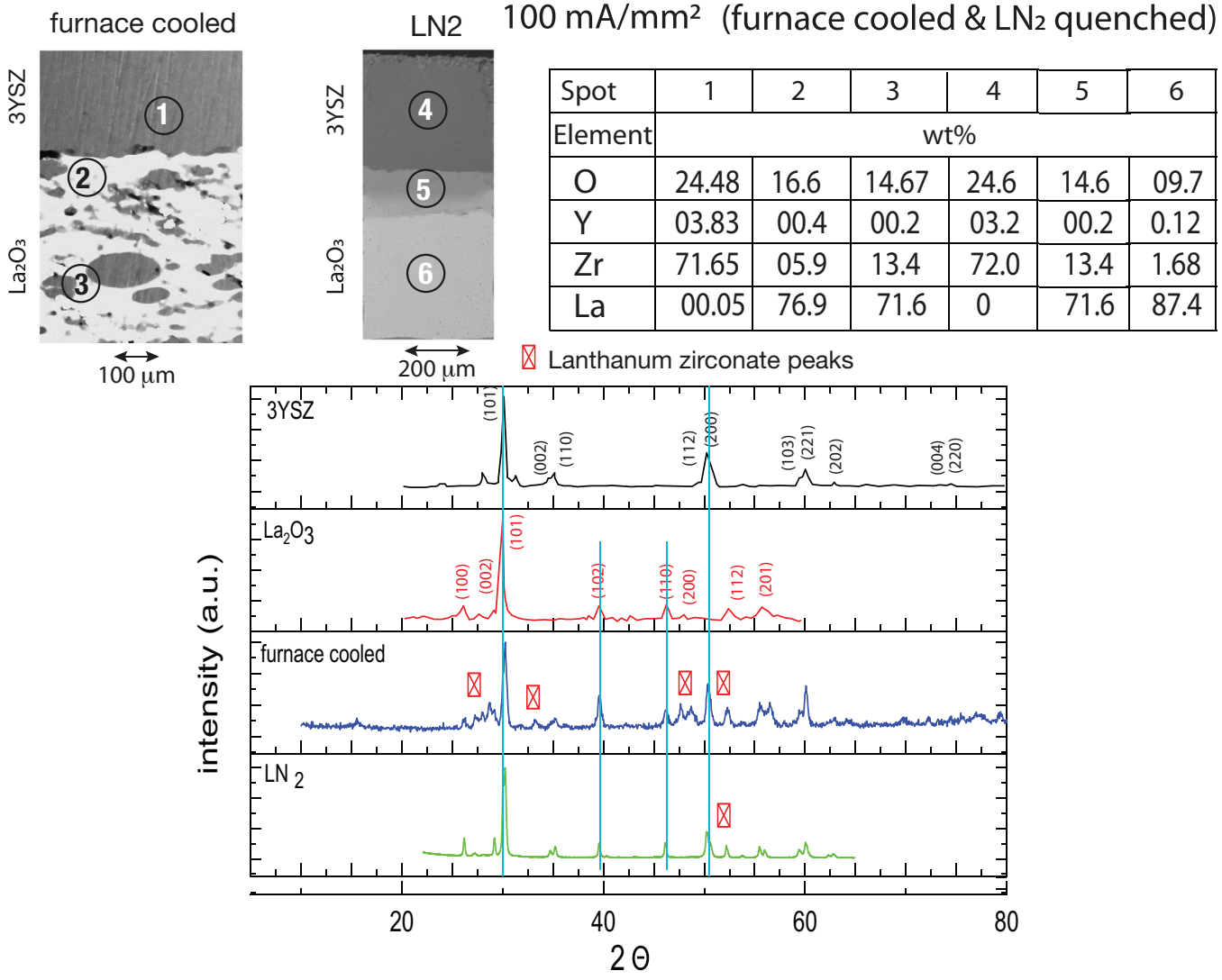

Spot	1	2	3	4	5	6
Element	wt%					
O	24.48	16.6	14.67	24.6	14.6	09.7
Y	03.83	00.4	00.2	03.2	00.2	0.12
Zr	71.65	05.9	13.4	72.0	13.4	1.68
La	00.05	76.9	71.6	0	71.6	87.4

FIGURE 9 EDS and X-ray diffraction data from furnace-cooled and LN_2-quenched samples

The question then arises if a lattice expansion of about 3% can account for the very large increase in the diffusion rate as measured in the present experiments (relative to conventional diffusion). In metals, the transition from the solid to the molten state (at the same temperature) is accompanied by a volumetric expansion of 3%, and an increase in the diffusion coefficient by three orders of magnitude.[26] Thus, to some extent, the increase in diffusion rate, measured presently, may be attributed to lattice expansion. However, the increase in the flash experiment is far larger, nearly seven orders of magnitude. It is possible that large amplitude lattice vibrations as reported from diffuse scattering data analyzed by the pair–distribution–function method[30] may contribute to rapid diffusion, as well. These large amplitudes may also induce unusual lattice expansion. Most likely, both the lattice expansion and a resonance between lattice vibrations and the jump frequency of atoms are the underlying cause of the "super" diffusion rate in flash.

Recent work on touch-free sintering where flash can be transmitted from an active specimen to a passive powder-pressed sample, without attachment of electrodes, by magnetic induction, suggests the state of flash to have the nature of a solid-state plasma. The lattice vibrations in a plasma are likely to have large amplitudes that can expand the lattice and may lead to faster diffusion.

The higher specific volumes in flash-Stage III may also explain the flattening of the activation barrier for diffusion, as described in this article.

It is also noteworthy that the sintering kinetics during flash are estimated to be four-to-five orders of magnitude faster than anticipated from the Arrhenius extrapolation of data from conventional sintering. Sintering in yttria-stabilized zirconia is controlled by cation diffusion.

ACKNOWLEDGMENTS

We are grateful to the Office of Naval Research for supporting this research under the Grant no. N00014-18-1-2270 under the direction of Dr. Antti Makinen. Movie Caption (Supporting Information) Live liquid nitrogen immersion of in-flash bilayer specimen.

ORCID

Rishi Raj https://orcid.org/0000-0001-8556-9797

REFERENCES

1. Yu M, Grasso S, Mckinnon R, Saunders T, Reece MJ. Review of flash sintering: materials, mechanisms and modelling. Adv Appl Ceram. 2017;116(1):24–60. https://doi.org/10.1080/17436753.2016.1251051
2. Raj R. Analysis of the power density at the onset of flash sintering. J Am Ceram Soc. 2016;99(10):3226–32. https://doi.org/10.1111/jace.14178
3. Jones GM, Biesuz M, Ji W, John SF, Grimley C, Manière C, et al. Promoting microstructural homogeneity during flash sintering of ceramics through thermal management. MRS Bull. 2021;46(1):59–66. https://doi.org/10.1557/s43577-020-00010-2
4. Biesuz M, Sglavo VM. Flash sintering of alumina: effect of different operating conditions on densification. J Eur Ceram Soc. 2016;36(10):2535–42. https://doi.org/10.1016/j.jeurceramsoc.2016.03.021
5. Guillon O, Gonzalez-Julian J, Dargatz B, Kessel T, Schierning G, Räthel J, et al. Field-assisted sintering technology/spark plasma sintering: mechanisms, materials, and technology developments. Adv Eng Mater. 2014;16(7):830–49. https://doi.org/10.1002/adem.201300409
6. 6 papers. Synthesis and Processing Under Electric/Electromagnetic Fields. MRS Bull. 2021;46.
7. Gil-González E, Pérez-Maqueda LA, Sánchez-Jiménez PE, Perejón A. Flash sintering research perspective: a bibliometric analysis. Materials. 2022;15(2):416. https://doi.org/10.3390/ma15020416
8. Francis JSC, Raj R. Influence of the field and the current limit on flash sintering at isothermal furnace temperatures. J Am Ceram Soc. 2013;96(9):2754–8. https://doi.org/10.1111/jace.12472
9. Kumar MKP, Yadav D, Lebrun J-M, Raj R. Flash sintering with current rate: a different approach. J Am Ceram Soc. 2019;102(2):823–35. https://doi.org/10.1111/jace.16037
10. Cross L, Raj R, Jalali SIA. On the catalytic effect of zirconia on flash sintering of alumina. J Am Ceram Soc. 2022;105(6):3746–52. https://doi.org/10.1111/jace.18423
11. Gil-González E, Perejón A, Sánchez-Jiménez PE, Sayagués MJ, Raj R, Pérez-Maqueda LA. Phase-pure $BiFeO_3$ produced by reaction flash-sintering of Bi_2O_3 and Fe_2O_3. J Mater Chem A. 2018;6(13):5356–66. https://doi.org/10.1039/C7TA09239C
12. Avila V, Raj R. Reactive flash sintering of powders of four constituents into a single phase of a complex oxide in a few seconds below 700°C. J Am Ceram Soc. 2019;102(11):6443–8. https://doi.org/10.1111/jace.16625
13. Huang X, Tang J, Zhou Y, Rui K, Ao X, Yang Y, et al. Developing preparation craft platform for solid electrolytes containing volatile components: experimental study of competition between lithium loss and densification in $Li_7La_3Zr_2O_{12}$. ACS Appl Mater Interfaces. 2022;14(29):33340–54. https://doi.org/10.1021/acsami.2c08442
14. Wakai F, Sakaguchi S, Matsuno Y. Superplasticity of yttria-stabilized tetragonal ZrO_2 polycrystals. Adv Ceram Mater. 1986;1(3):259–64.
15. Motomura H, Tamao D, Nambu K, Masuda H, Yoshida H. Athermal effect of flash event on high-temperature plastic deformation in Y_2O_3-stabilized tetragonal ZrO_2 polycrystal. J Eur Ceram Soc. 2022;42(12):5945–52. https://doi.org/10.1016/j.jeurceramsoc.2022.04.055
16. Kathiria RK, Jo, S, Raj, R, Yadav, D. In-flash immersion-and-quench of yttria-stabilized zirconia into liquid nitrogen yields an electronic conductor. J Am Ceram Soc. 2021;105:1635–9.
17. Terauds K, Lebrun J-M, Lee H-H, Jeon T-Y, Lee S-H, Je JH, et al. Electroluminescence and the measurement of temperature during Stage III of flash sintering experiments. J Eur Ceram Soc. 2015;35(11):3195–9. https://doi.org/10.1016/j.jeurceramsoc.2015.03.040
18. Yadav D, Raj R. Two unique measurements related to flash experiments with yttria-stabilized zirconia. J Am Ceram Soc. 2017;100(12):5374–8. https://doi.org/10.1111/jace.15114
19. Bordia RK, Raj R. Sintering behavior of ceramic films constrained by a rigid substrate. J Am Ceram Soc. 1985;68(6):287–92. https://doi.org/10.1111/j.1151-2916.1985.tb15227.x
20. Jha SK, Raj R. Electric fields obviate constrained sintering. J Am Ceram Soc. 2014;97(10):3103–9. https://doi.org/10.1111/jace.13136
21. Cheng T, Raj R. Flaw generation during constrained sintering of metal-ceramic and metal–glass multilayer films. J Am Ceram Soc. 1989;72(9):1649–55.
22. Francis JS, Cologna M, Montinaro D, Raj R. Flash sintering of anode–electrolyte multilayers for SOFC applications. J Am Ceram Soc. 2013;96(5):1352–4.
23. Jalali SIA, Raj R. Touch-free flash sintering with magnetic induction within a reactor activated by the usual flash method. J Am Ceram Soc. 2022;105(11):6517–22. https://doi.org/10.1111/jace.18601
24. Shewmon PG. Diffusion in solids. New York: McGraw-Hill; 1963
25. Kilo M, Borchardt G, Lesage B, Kaıtasov O, Weber S, Scherrer S. Cation transport in yttria stabilized cubic zirconia: 96Zr tracer diffusion in $(Zr_xY_{1-x})O_{2-x/2}$ single crystals with $0.15 \leqslant x \leqslant 0.48$. J Eur Ceram Soc. 2000;20(12):2069–77.
26. Battezzati L, Greer AL. The viscosity of liquid metals and alloys. Acta Metall. 1989;37(7):1791–802. https://doi.org/10.1016/0001-6160(89)90064-3
27. Lebrun J-M, Hellberg CS, Jha SK, Kriven WM, Steveson A, Seymour KC, et al. In-situ measurements of lattice expansion related to defect generation during flash sintering. J Am Ceram Soc. 2017;100(11):4965–70. https://doi.org/10.1111/jace.15071
28. Goodrich WE. Volume changes during the solidification of metals and alloys of low melting-point. Trans Faraday Soc. 1929;25:531–69.
29. Wassel MAB, Pérez-Maqueda LA, Gil-Gonzalez E, Charalambous H, Perejon A, Jha SK, et al. Anisotropic lattice expansion determined during flash sintering of $BiFeO_3$ by in-situ energy-dispersive X-ray diffraction. Scr Mater. 2019;162:286–91. https://doi.org/10.1016/j.scriptamat.2018.11.028
30. Yoon B, Yadav D, Raj R, Sortino E, Ghose S, Sarin P, et al. Measurement of O and Ti atom displacements in TiO_2 during

flash sintering experiments. J Am Ceram Soc. 2018;101(5):1811–7. https://doi.org/10.1111/jace.15375

SUPPORTING INFORMATION

Additional supporting information can be found online in the Supporting Information section at the end of this article.

How to cite this article: Jalali SIA, Raj R. Reactive flash sintering in a bilayer of zirconia and lanthana: Measurement of the diffusion coefficient in real time. J Am Ceram Soc. 2023;106:867–877. https://doi.org/10.1111/jace.18804